Mon. Not. R. Astron. Soc. **305,** 957–965 (1999)

The bulk expansion of the supernova remnant Cassiopeia A at 151 MHz

M. A. Agüeros and D. A. Green
Mullard Radio Astronomy Observatory, Cavendish Laboratory, Madingley Road, Cambridge CB3 0HE

Accepted 1999 January 25. Received 1998 December 30; in original form 1998 July 29

ABSTRACT

We present observations of the supernova remnant Cassiopeia A made over 13 yr at 151 MHz with the Cambridge Low-Frequency Synthesis Telescope. These observations have been used to study the contraction of well-defined minima in the visibility (or u, v) plane, in order to determine the bulk expansion of the radio emission from Cas A. These observations show steady contraction of the first and second minima, corresponding to expansion time-scales of ~400–500 yr. These time-scales are less than those inferred from the expansion of compact radio knots in Cas A, and imply, provided that shape changes are not significant, that the remnant is in the transition between free expansion and Sedov–Taylor phases.

Key words: techniques: interferometric – ISM: individual: Cas A – supernova remnants – radio continuum: ISM.

1 INTRODUCTION

Cassiopeia A (Cas A) is one of the brightest radio sources in the sky, and is the youngest (~300 yr old) supernova remnant (SNR) identified in our Galaxy. Because it is so young, observations made over several years allow its dynamics to be studied in detail. In general, young shell SNRs such as Cas A are initially expected to be in a free or undecelerated expansion stage, when they have not swept up much mass. In this phase radius ∝ age, and the age of the remnant is equal to the dynamical age, i.e. the age that is deduced assuming the *current* expansion speed of the remnant. As SNRs sweep up an appreciable amount of material, and decelerate, they move into the Sedov–Taylor phase, where radius ∝ age$^{2/5}$ (see for example Woltjer 1970). In this phase the dynamical age is 5/2 times the true age.

The age of Cas A has been deduced from the proper motions of compact optical features, which are thought to be very dense and therefore undecelerated 'bullets' of material ejected during the SN event. Table 1 summarizes the deduced date of the SN that produced Cas A from such optical studies, all of which place the origin of Cas A in the late seventeenth century (which is consistent with the date of the possible sighting by John Flamsteed; see Ashworth 1980).

At radio wavelengths, studies of the expansion of Cas A have mostly been based on the proper motions of well-defined, bright, compact 'knots' seen in radio images (see Table 2). These studies show a dynamical time-scale of ~900–950 yr, several times that found from the dense optical knots, which implies that the radio knots have been greatly decelerated. However, it is unlikely that the dynamical age of Cas A deduced from the radio knots is representative of the overall dynamical age of the radio emission from the remnant, as the compact radio features represent only a small – and possibly biased – fraction of the total emission from the remnant.

An alternative method, as introduced by Green (1988), has been used to study the expansion of the bulk radio emission from Cas A. This involves measuring the contraction rate of well-defined minima in the amplitude of the visibility function as observed with a radio interferometer. Two such studies have been made, but with inconsistent results (see Table 2). Although Green (1988) deduced a dynamical age of ~400 yr – closer to that obtained from the studies of proper motions of the optical knots than that obtained from studies of the radio knots – Anderson & Rudnick (1995) derived a dynamical age closer to that which they deduced from the radio knots (their results also varied with position angle). However, these two studies were based on the contraction of different features in the visibility (or u, v) plane, using different comparison methods, and were made at frequencies differing by a factor of about 10. In addition, Green's results were based on the contraction of only the first minimum in the u, v plane, and therefore could not take into account the possibility of changes in the shape of the emission from Cas A.

In order to investigate the bulk expansion of Cas A further, to try to resolve the apparent inconsistency noted above, and to constrain the significance of any shape changes on the derived results, we have made further studies of the contraction of well-defined features in the visibility plane. We had at our disposal observations of Cas A taken with the Cambridge Low-Frequency Synthesis Telescope (CLFST) over a period of approximately 13 years at 151 MHz. These studies have two main advantages over those made by Green (1988): (i) more than just two epochs are used, so that it is possible to see if a steady contraction rate for a given feature occurs, and (ii) the contractions of two minima in the visibility plane have been studied, as a check on the significance of any shape changes on the measured dynamical age of Cas A.

Table 1. Date for the Cas A SN from studies of the proper motions of optical features.

Author(s)	Estimated SN date
van den Bergh & Dodd (1970)	1667 ± 8
Kamper & van den Bergh (1976)	1657 ± 3
Fesen, Becker & Goodrich (1988)	1680

Table 2. Radio expansion studies of Cas A.

Author(s)	Features, frequency	Period of observations	Fractional change /per cent yr^{-1}	Dynamical age/yr
Bell (1977)	Knots, 5 GHz	1969–74	0.11	918
Tuffs (1986)	Knots, 5 GHz	1974–78	0.10 to 0.11	949^{+44}_{-41}
Anderson & Rudnick (1995)	Knots, 1.5 and 5 GHz	1978–91	0.10	∼950
Green (1988)	First minimum in the u, v plane, 151 MHz	1984–86	0.22 to 0.26	∼400
Anderson & Rudnick (1995)	Features in the u, v plane, 1.5 GHz	1985–90	0.07 to 0.13	750 to 1300

2 OBSERVATIONS

Cas A was observed with the CLFST on many occasions between 1984 and 1997, and 10 good-quality observations were selected for analysis. The characteristics of the CLFST, an east–west aperture synthesis, Earth rotation instrument, are summarized in Table 3 (for a more detailed description, see Rees 1989 or McGilchrist et al. 1990). An observation typically consisted of 1440 30-s integrations, or 'samples' (see Table 4). An example of a synthesized image of Cas A from one of these observations is shown in Fig. 1. The observations were edited and calibrated, as summarized below (a detailed description of this process is given in Agüeros 1997).

First, bad data were identified and removed from the observations. Several factors could be responsible for producing these data. A few samples (at most 4.5 per cent of the total) at the beginning of some observations were removed as some antennas were still slewing to Cas A. Other samples within the observations were affected by interference. Occasionally, individual antennas were not functioning correctly throughout certain observations. As the CLFST has many antennas and baselines, omitting a malfunctioning antenna or two from the data does not significantly affect it. The u, v planes produced here averaged the 776 baselines into about 120 cells, so that each cell contained the information of six or seven baselines. Also, since each observation consisted of over 1400 samples, removing a few poor samples because of interference did not limit the coverage in the u, v plane greatly.

Secondly, before some of the analysis could be made of the contraction of features in the u, v plane, the relative amplitudes of the observations had to calibrated. This was necessary not only because of the intrinsic fading of Cas A, but also because the sensitivity of the CLFST has been decreasing with time, by ∼1 per cent a year (Riley, private communication). The averaged amplitude response of the first 100 baselines at each epoch was used as a measure of the total flux density of Cas A (see Fig. 2). Before making the annular analysis (see later discussion), the aperture planes from each epoch were scaled so that the apparent flux density was the same.

Interferometric observations at 151 MHz are badly affected by phase variations induced by the ionosphere. For most observations made with the CLFST, corrections can be made by 'self-calibration' using a compact and bright source in the same field of view. This is not feasible for observations of Cas A, as it is itself so bright. As a result, comparisons of images of Cas A made with the CLFST would be limited by errors in the phase calibration. In addition, it is not possible to define the extent of the remnant uniquely. A method that is not sensitive to ionospheric phase uncertainties is therefore preferable for determining the bulk expansion of Cas A. Here we analyse the amplitudes of the observed visibilities (following Green 1988).

Table 3. Characteristics of the CLFST.

Observing frequency[a]	151 MHz
Antenna	4×10-element yagis
Primary beam (FWHM)	17°
Mount	equatorial
Number of antennas	60
Baseline interval	3λ (∼6 m)
Maximum baseline	779 (×3λ = 4.6 km)
Number of baselines	776
Missing baselines	0, 1, 3, 778
Beamwidth	$70 \times 70\,\mathrm{cosec}(\delta)$ arcsec^2
Bandwidth[a]	700 kHz
Typical noise (12-h synthesis)	20 mJy beam^{-1}

[a]In 1988, the observing frequency was changed from 151.5 to 151.0 MHz, and the bandwidth reduced from 800 to 700 kHz.

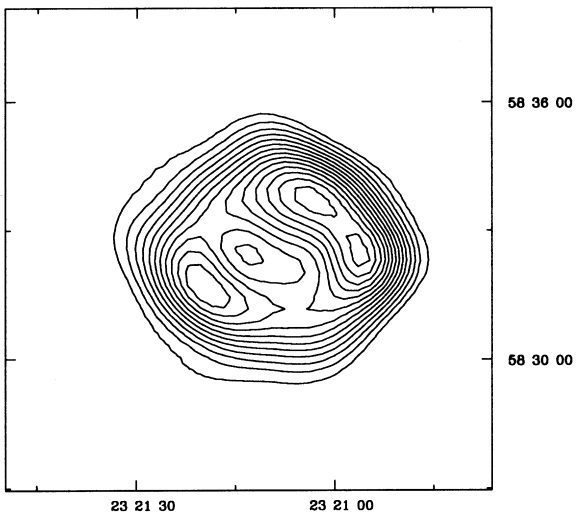

Figure 1. Cas A at 151 MHz, from 1986/Apr/20 observation. The contours are linearly spaced, and the coordinates are B1950.0.

Table 4. The selected observations of Cas A made with the CLFST.

Epoch	Corrections	Range of samples (Integration time)	Equivalent observation time
1984/Jul/18[a]	Samples 1–16, 117–121, 1240–1256, 1270–1280, 1345–1349, 1411–1440 removed		
	Aerial 33 removed	17–1410 (30 s)	11.3 h
1984/Aug/09	Samples 1–13, 1206–1214 removed	14–1230 (30 s)	10.1 h
1986/Apr/20	None	1–1440 (30 s)	12.0 h
1986/Oct/01[a]	Samples 268–318, 338–345, 352–359, 380–382, 435–454, 483–485, 494–520,		
	529–531, 543, 550, 561–581, 587–637, 646–658, 892–895, 912–914 removed	1–1425 (30 s)	9.9 h
1987/Aug/19	Samples 1–16 removed	17–1440 (30 s)	11.9 h
1988/Oct/13	Samples 693–698, 1181–1350 removed		
	Aerial 13 removed	1–1180 (32 s)	10.5 h
1990/Sep/21	Samples 1–60, 163–166, 874–876, 882–889 removed		
	Aerials 13 and 29 removed	61–1350 (32 s)	11.4 h
1993/Oct/18	Samples 1–20, 22, 24, 27–31, 33–34, 94–103, 1441 removed		
	Aerial 44 removed	21–1440 (30 s)	11.7 h
1997/May/12	Samples 1031–1039, 1441 removed		
	Aerial 23 removed	1–1440 (30 s)	11.9 h
1997/Aug/09	Aerial 28 removed	1–1440 (30 s)	12.0 h

[a] These two observations were used in Green (1988), although the second was mis-labelled as 1986/Nov/01.

At radio wavelengths, Cas A appears as an irregular ring – the projection of a shell – about 5 arcmin in diameter (e.g. Bell 1977; see Fig. 1). If this shell were symmetric, we would expect to find two circular amplitude zeros in the area of the u, v plane observed with the CLFST. As the shell is asymmetric, we instead find two amplitude minima in the u, v planes (see Fig. 3). If Cas A is expanding uniformly, measuring the expansion rate of the remnant can be done simply by measuring the contraction rate of either of the minima in the u, v plane (e.g. Green 1988, who measured the contraction rate of the first minimum only). However, if the remnant is undergoing a shape change, evaluating the expansion rate requires analysis of the contraction of both minima in the u, v plane, along with a discussion of possible models for such a change (see later discussion). We therefore evaluate the contraction rate of both minima in the u, v planes as measured by the CLFST.

We analysed the data in two different ways. For the first method – the 'annular analysis' – an annulus within the u, v planes containing one of the two minima was identified, and a statistical misfit between the amplitudes in this annulus for each of the aperture planes of a given epoch and the corresponding annulus in a reference aperture plane was used. For the second method – the 'positional analysis' – the amplitude functions of each u, v plane were azimuthally averaged, and then the positions of the minima in these functions were fitted.

3 RESULTS

3.1 Annular analysis

For this analysis, the 1990/Sep/21 observation was used for reference. This is a good-quality data set close to the mid-point of the 13-yr time-span of our observations. We also chose 40.0 arcsec/pixel as the scaling of an image corresponding to this reference aperture plane, which is equivalent to a cell size of about 20λ in the u, v plane. This choice ensured that the number of baselines averaged into each cell of the aperture plane was between six and seven, so that the removal of data from malfunctioning antennas (as discussed earlier) does not result in empty cells in the u, v planes.

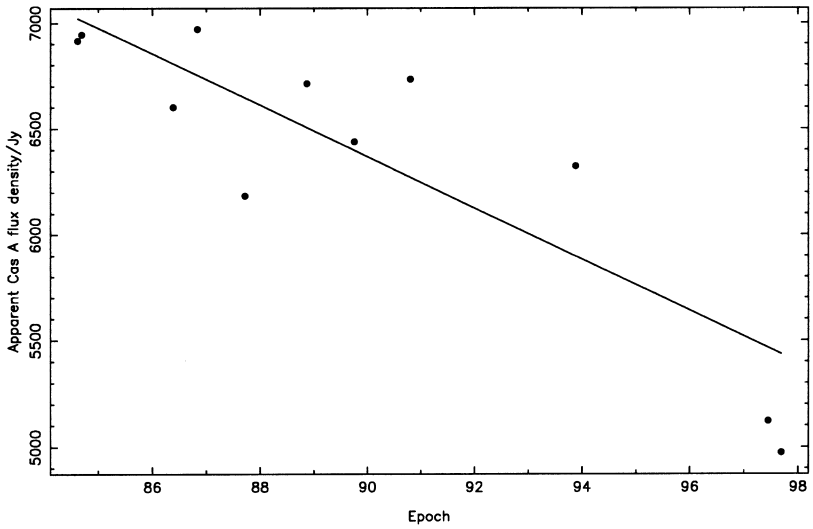

Figure 2. The apparent flux density of Cas A over time, not corrected for the sensitivity decrease of the CLFST. The values for each epoch are obtained by averaging the amplitudes of the smallest 100 baselines. Since the sensitivity of the telescope is reduced as the brightness temperature of the observed region of the sky increases, the apparent flux densities of Cas A are less than its absolute flux density.

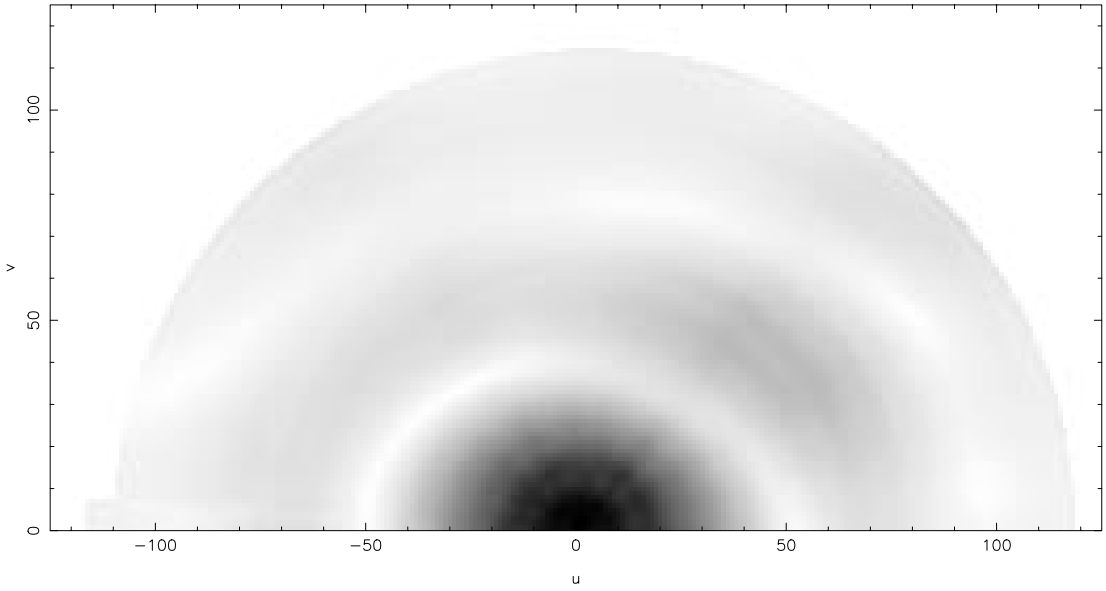

Figure 3. The observed visibility amplitude (black indicating higher amplitude) for an example u, v plane corresponding to an image with an angular scaling of 30.5 arcsec pixel^{-1}, from the 1986/Apr/20 observation.

For each other epoch, we then made a series of seven u, v planes corresponding to images with slightly larger or smaller angular scalings. Since Cas A expands over time, aperture planes made from observations taken before 1990/Sep/21 were contracted (i.e., the corresponding images were expanded by making them with angular scalings smaller than 40.0 arcsec pixel^{-1}) in order to match features in the reference aperture plane. Similarly, aperture planes from later observations were expanded; in this way, for each observation, we produced a series of regularly spaced aperture planes (for example, corresponding to images with an angular scaling of 40.3, 40.4, 40.5 arcsec pixel^{-1}, etc., for a later epoch) to compare to the reference aperture plane.

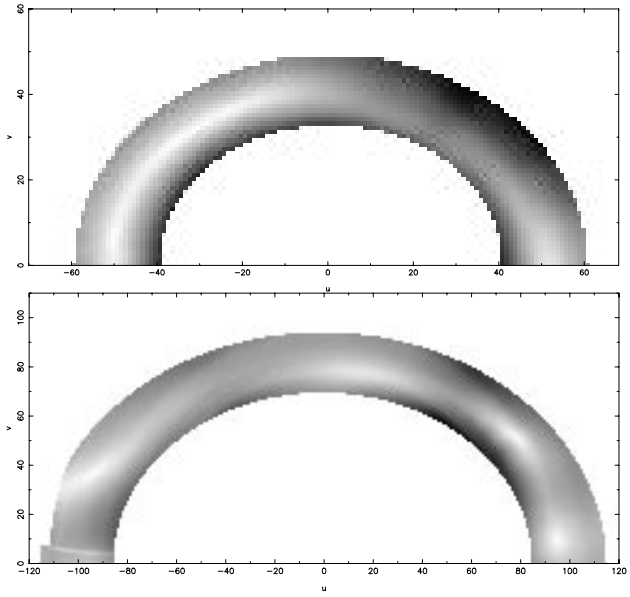

Figure 4. The amplitude of the observed visibility function near the first (top) and second (bottom) minima (black indicating higher amplitude, with different scalings for each minimum). Both minima are from the 1986/Apr/20 observation aperture plane presented in Fig. 3.

Although Cas A is very nearly circular on the sky, the position of the remnant ($\delta \sim 58°$) creates elliptical minima in the u, v planes obtained with the CLFST. For comparisons of a u, v plane at a given epoch with that of the reference epoch, elliptical annuli were defined. A scaled radius R from the origin to the centre of each cell in the u, v plane was calculated:

$$R = \sqrt{x^2 + 1.5y^2}, \tag{1}$$

where x and y are the u and v coordinates of a cell of the aperture plane; the factor of 1.5 was found to produce annuli that traced the minima well (see Fig. 4). For every cell in both aperture planes for which data existed, and for which $R_1 \leq R \leq R_2$, a simple statistical misfit was calculated between the amplitude from the reference 1990/Sep/21 aperture plane and that at the same cell in annuli from aperture planes of other epochs. This misfit was calculated as:

$$\frac{1}{N}\sum_{i=1}^{N}\left(\frac{A(i)_{\rm ref}}{A(i)_{\rm epoch}} - 1\right)^2, \tag{2}$$

where N is the number of valid cells in the annulus, and $A(i)_{\rm ref}$ and $A(i)_{\rm epoch}$ are the amplitudes for the ith cell in the reference aperture plane and in the aperture plane being compared, respectively. This statistic scales the difference in amplitude between the two cells being compared, rendering it more sensitive to differences near the amplitude minima and less sensitive to differences in the larger amplitude values at the edges of the compared annuli. This differs from the least-squares method employed by Green (1988), and from the statistic used by Anderson & Rudnick (1995).

For each epoch the misfit statistic was calculated for comparisons of the reference aperture plane with the seven aperture planes corresponding to the various angular scalings. These misfit values were then fitted by a second-order polynomial function of the angular scale to find which scaling produced the minimum misfit (see Fig. 5). The contraction rate of the minimum in the u, v plane between the two epochs was calculated from the change between the scaling of the u, v plane for which the misfit was minimized for that epoch and that of the reference 1990/Sep/21 u, v plane.

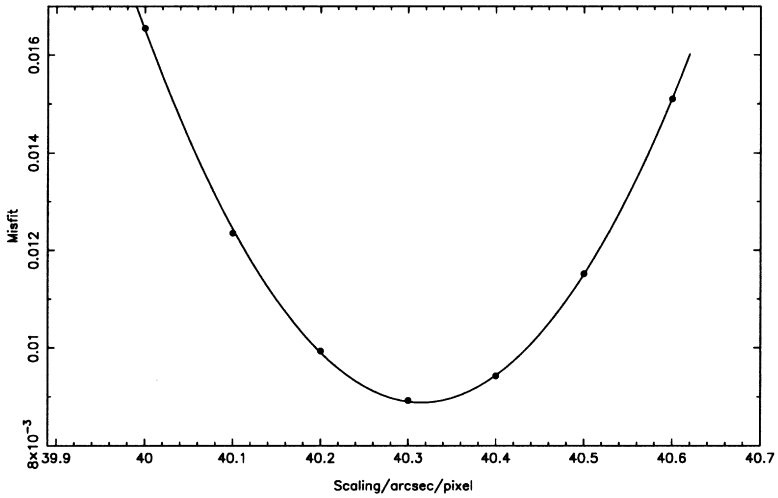

Figure 5. An example of how the minimum misfit is obtained from the annular analysis. The data points are the calculated misfit values between the annulus containing the first minimum for each 1993/Oct/18 u, v plane and the reference 1990/Sep/21 u, v plane. The line is the best-fitting second-order polynomial to the data.

The dependence of the results obtained on the chosen radial range for the annuli, and on the applied amplitude scaling, was investigated, as the minima are not symmetric. We found that variations in the radial range used to define the annuli, as long as these included and traced the minimum, changed the deduced scaling for the minimum misfit by at most ~0.03 per cent. We varied the amplitude scaling by up to 10 per cent, and found that the scaling of the best fit was changed by at most ~0.03 per cent.

Two of the aperture planes were missing coverage over 2 h of the observations: for 1984/Aug/09, the first 2 h were missing; for 1988/Oct/13, it was the last 2 h. As a result, these two data sets are biased in position angle relative to the other observations, as they both exclude a large section of the u, v planes from comparison. Therefore care had to be taken with the results obtained with these observations.

Table 5. Results of annular analysis.

	First minimum		Second minimum	
Epoch	Scaling of best fit /arcsec pixel^{-1}	Change /per cent	Scaling of best fit /arcsec pixel^{-1}	Change /per cent
1984/Jul/18	39.36	+1.61	39.57	+1.07
1984/Aug/09[a]	39.50	+1.25	39.73	+0.67
1986/Apr/20	39.54	+1.15	39.58	+1.09
1986/Oct/01	39.62	+0.95	39.79	+0.53
1987/Aug/19	39.60	+1.00	39.76	+0.61
1988/Oct/13[a]	39.84	+0.40	39.89	+0.26
1993/Oct/18	40.32	−0.79	40.16	−0.40
1997/May/12	40.58	−1.44	40.60	−1.49
1997/Aug/09	40.69	−1.72	40.67	−1.66
	Scaling of u, v plane used to calculate per cent change			
1990/Sep/21	40.00		40.00	

[a]These two data sets contained 2-h gaps in the u, v planes.

Table 6. Contraction rate of minima in the u, v plane and deduced dynamical age, from annular analysis.

	Contraction rate/per cent yr^{-1}	Deduced dynamical Cas A age/yr
First minimum	0.247 ± 0.015	405^{+26}_{-23}
Second minimum	0.202 ± 0.013	496^{+33}_{-31}

For the first minimum, the annuli were defined from $R_1 = 40$ to $R_2 = 60$. For the second minimum, the annuli were defined from $R_1 = 85$ to $R_2 = 115$. In general, the second minimum was far less sharply defined than the first, requiring the use of a wider annulus to trace it over the course of an observation. Fig. 4 shows examples of the first and second minima isolated using these definitions for the annuli.

Table 5 presents the annular analysis results, which are displayed in Fig. 6, for both the first and the second minima. For each minimum, the data are well fitted by a straight line, corresponding to a linear contraction of the minima in the u, v plane, and suggesting that the effects of any uncertainties are small. Assuming that Cas A is expanding uniformly, the dynamical age of the remnant can be straightforwardly calculated from the contraction rate obtained by the fitting (excluding the two epochs significantly less than 12 h long). Table 6 presents the results for the contraction rate and corresponding dynamical age. The errors were estimated from the use of a range of reasonable linear fits, determined by eye, to the data.

3.2 Positional analysis

To obtain the average position of a minimum, an azimuthally averaged amplitude function was calculated for each u, v plane, using the non-circular coordinate system defined previously to trace the minima. The azimuthally averaged amplitude at a scaled radius R was calculated as the average of the amplitudes of all cells in the u, v plane at radii between $R - 1/2$ and $R + 1/2$. Fig. 7 shows an example of the azimuthally averaged amplitudes for 1986/Apr/20, and a detail of the fitting of the first minimum. All seven of the aperture planes produced for an epoch were used; this allowed us to estimate the uncertainty in the average position of a minimum for an epoch, from the scatter of the individual values found for the fitted minima.

The results for this analysis are given in Table 7. The first two columns are the results obtained for both minima for the seven epochs for which complete, or nearly complete, 12-h observations were available. The last two columns of Table 7 give the results for nine of the 10 epochs, for an analysis limited to 8 h of observing time (equivalent to 120° of the u, v plane). One observation, 1986/Oct/01, was entirely set aside from this analysis;

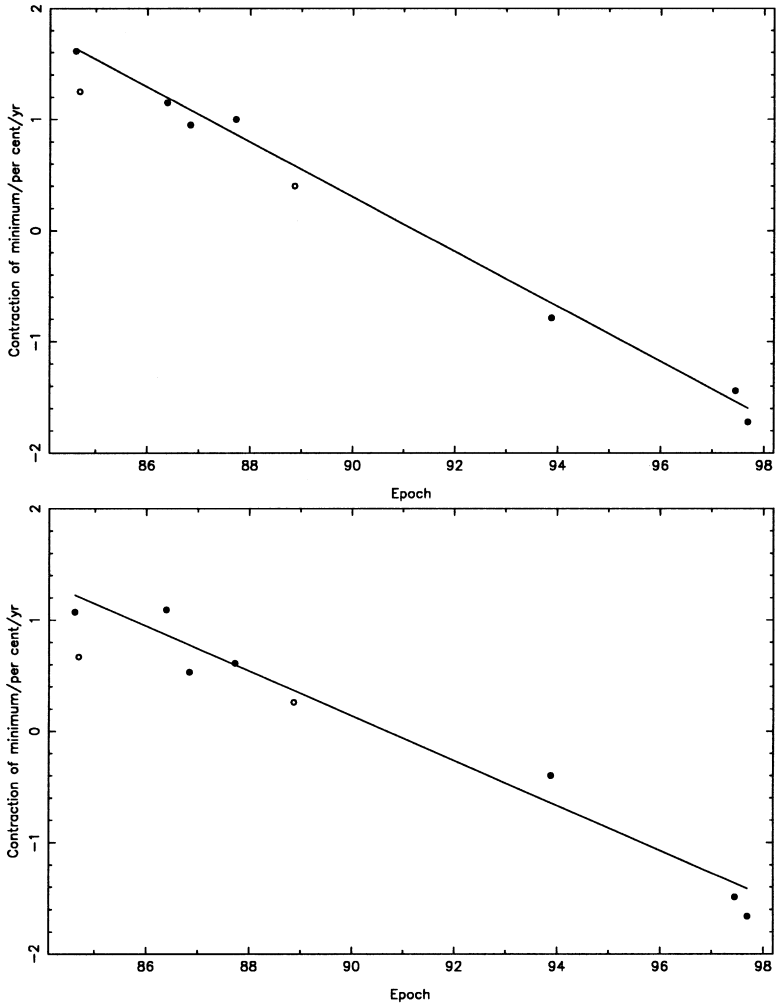

Figure 6. The results obtained by the annular analysis. The top plot is for the first minimum, and the bottom plot is for the second minimum. The open circles indicate the two data sets with significant gaps; these points were excluded when fitting. The slope of the straight-line fit in each case provides a measure of the contraction of the features in the u, v plane over time.

the removal of bad samples created gaps in the aperture plane at position angles that made it difficult to select a suitable range for which the observation could be included. The average positions of the minima are given in 'reference cells' (R.C.), positions in the amplitude plane corresponding to an image made with an angular scaling of 40.0 arcsec pixel^{-1}. Fig. 8 presents the results for the 12-h observations. As before, the best straight-line fit to the data gives the average contraction rate of the minima in the u, v plane. The contraction rates and equivalent dynamical ages deduced are listed in Table 8 for the 12-h observations. The results obtained using the 8-h observations are similar for the first minimum; for the second minimum, we find a slightly greater dynamical age.

Table 7. Results of positional analysis.

	Twelve-hour observations		Eight-hour observations	
Epoch	First minimum position/R.C.[a]	Second minimum position/R.C.	First minimum position/R.C.	Second minimum position/R.C.
1984/Jul/18	50.01 ± 0.03	100.16 ± 0.05	49.67 ± 0.04	99.93 ± 0.01
1984/Aug/09			49.68 ± 0.04	99.93 ± 0.02
1986/Apr/20	49.93 ± 0.03	99.69 ± 0.01	49.50 ± 0.04	99.45 ± 0.01
1987/Aug/19	49.64 ± 0.03	99.48 ± 0.05	48.19 ± 0.03	99.29 ± 0.05
1988/Oct/13			48.97 ± 0.03	99.22 ± 0.03
1990/Sep/21	49.32 ± 0.06	99.18 ± 0.07	48.90 ± 0.02	98.86 ± 0.06
1993/Oct/18	48.99 ± 0.03	98.49 ± 0.09	48.51 ± 0.02	98.32 ± 0.07
1997/May/12	48.64 ± 0.02	97.93 ± 0.09	48.13 ± 0.02	97.87 ± 0.10
1997/Aug/09	48.44 ± 0.02	97.55 ± 0.06	47.91 ± 0.03	97.69 ± 0.09

[a]R.C. = 'reference cells' – see text.

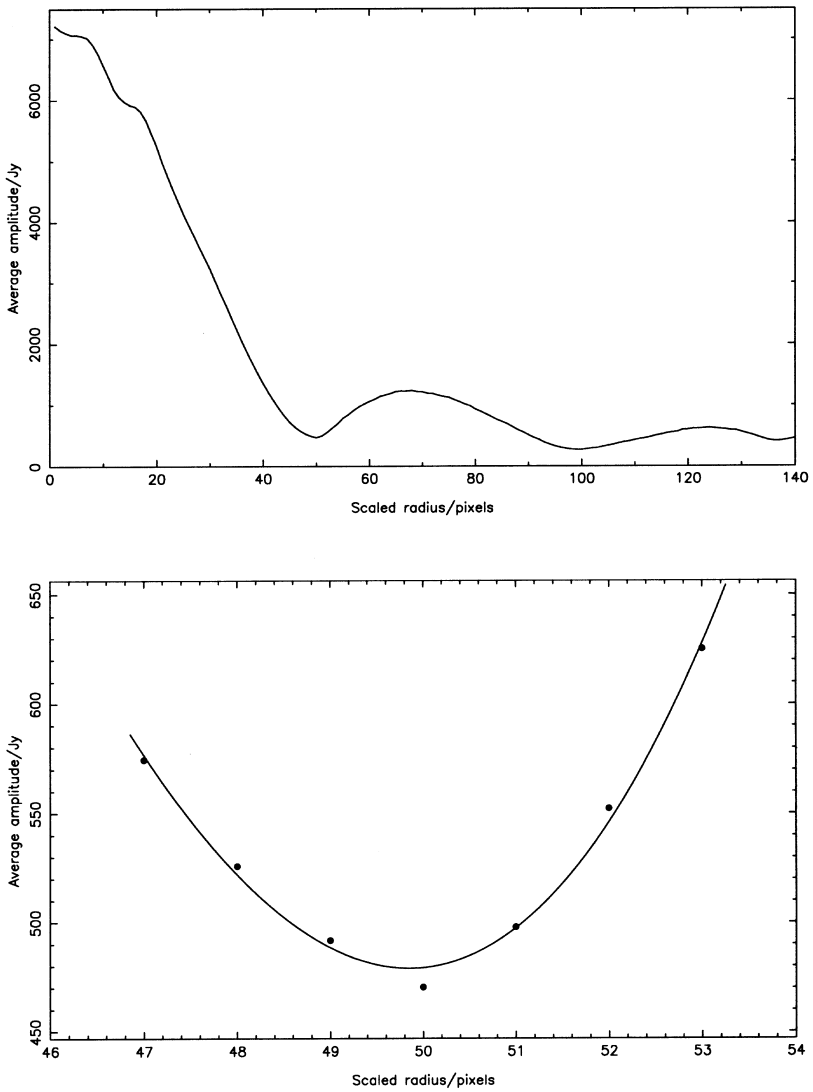

Figure 7. The azimuthally averaged amplitude (see text for details) of the observed visibility function for the 1986/Apr/20 u, v plane corresponding to an image with an angular scaling of 39.9 arcsec pixel^{-1}. The top plot shows the whole average, while the bottom plot shows the detail of the second-order fitting of the first minimum.

4 DISCUSSION AND CONCLUSIONS

Our analyses (Section 3) of the CLFST observations show that the positions of the first and second minima do contract in the visibility plane, and the results from the two methods show good agreement (Tables 6 and 8). A linear relation is sufficient to describe this contraction over the period 1984–1997, albeit at slightly different rates for each minimum. Combining the results from the annular and the positional (for the 12-h observations) methods, the dynamical ages associated with the contraction of the first and second minima are 406 ± 22 and 505 ± 22 years respectively. If Cas A was expanding in a self-similar way, we would expect these two time-scales to be the same. Our results therefore imply that there is some change in the shape of the emission of the remnant in addition to the overall expansion. In order to derive the rate of the expansion of the SNR, we modelled the influence of various changes in the shape of the shell on the obtained contraction rates for the two minima. The results of this simple modelling showed that, in the presence of shape changes (e.g. changing the radial width of the emission), the average contraction rate of the first two minima is a better estimate of the overall expansion of the remnant than that obtained from either the first or second minimum alone. Therefore, the average of the two dynamical ages – i.e. 460 ± 30 yr – is our best estimate of a characteristic dynamical age for the expansion of Cas A.

Table 8. Contraction rate of minima in the u, v plane and deduced dynamical age, from positional analysis for 12-h observations.

	Contraction rate/per cent yr^{-1}	Deduced dynamical age/yr
First minimum	0.244 ± 0.021	409^{+39}_{-32}
Second minimum	0.191 ± 0.014	522^{+43}_{-34}

This expansion time-scale is broadly consistent with the conclusions drawn by Green (1988), who found a dynamical age of about 400 years for Cas A, based on observations of only the first minimum at two epochs (see Table 2). However, it is quite different from the much larger dynamical time-scale of between 750 and 1300 years derived by Anderson & Rudnick (1995), also from contraction of features in the u, v plane. Their results and ours are difficult to compare directly, as the studies use different features in the u, v plane (Anderson & Rudnick used data out to the third

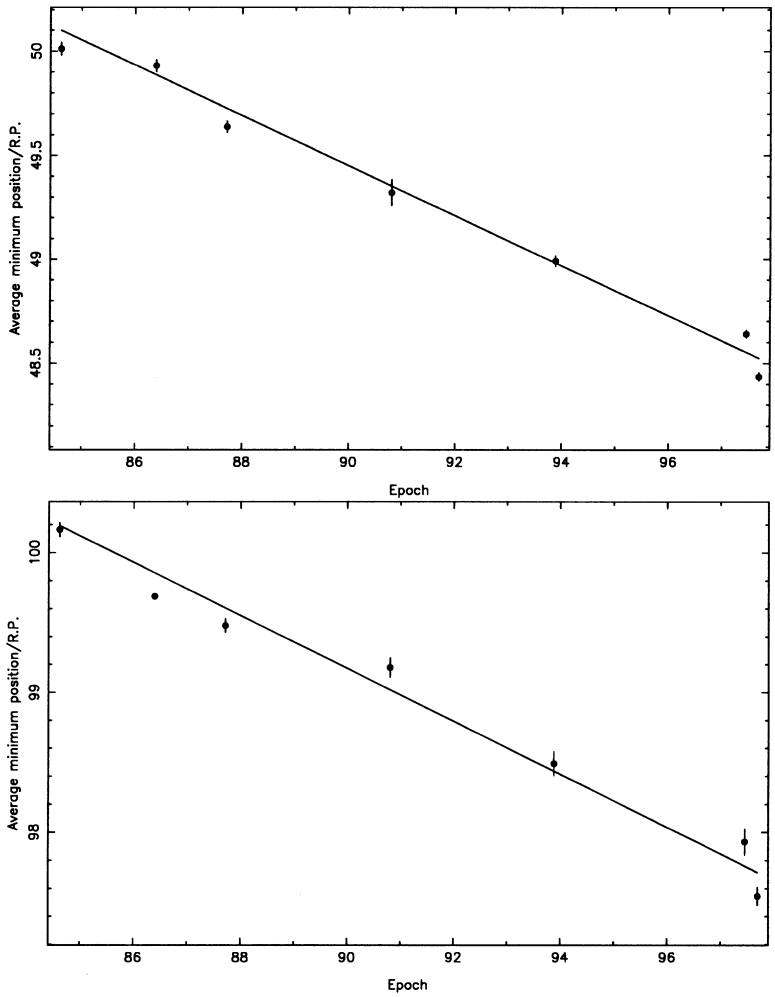

Figure 8. The evolution of fitted positions of the minima over time, calculated from the positional analysis using the seven epochs with close to 12-h observations. The line is the best straight-line fit (top – first minimum; bottom – second minimum).

minimum in the visibility function), different statistical comparisons, and quite different frequencies.

When compared to the true age of Cas A of 300 yr (see Section 1), our deduced dynamical age of ∼450 yr implies that it is in transition between the free expansion and Sedov–Taylor phases of evolution. This is consistent with the structure of the radio emission of Cas A, in which bright radio emission originates in the region of the contact discontinuity between the ejected and the swept-up material, which is Rayleigh–Taylor unstable (e.g. Gull 1973, 1975). In contrast, the measured radio expansion of the remnant of Tycho's SN of 1572 places it close to the Sedov–Taylor phase (Strom, Goss & Shaver 1982; Tan & Gull 1985), and the SNR appears as a smooth-edged shell of radio emission.

The low dynamical age for Cas A obtained from our observations is inconsistent with the results obtained by studies of the proper motions of the compact radio features of the remnant. Bell (1977), Tuffs (1986) and Anderson & Rudnick (1995) all found a dynamical time-scale for the expansion of the remnant of over 900 yr. However, our studies measure the bulk expansion of all the radio emission from Cas A, whereas the expansion studies of compact radio features are dependent on the dynamical behaviour of only a small fraction of the total radio emission from the remnant. The results of studies of the expansion time-scales of the compact features are therefore not representative of the overall expansion of Cas A. If the compact features – which may be decelerated ejecta, or swept-up interstellar medium (ISM) – are being caught up by the main shell then they must be moving more slowly than the main shell. Thus the compact feature will have a higher dynamical time-scale (as measured by Bell, and others) than the time-scale implied by the overall expansion of the remnant (as measured by us).

Recently, Vink et al. (1998) have studied the expansion of Cas A in X-rays, where most of the emission comes from the same region as does the bulk of the radio emission. These studies also find a dynamical age for the remnant shell between the age deduced from optical studies and the age deduced from studies of the strongly decelerated knots. This suggests, as does our study, that the remnant is in transition between the free expansion and Sedov–Taylor phases.

ACKNOWLEDGMENTS

MAA thanks the Euretta J. Kellett Fellowship for making his time at MRAO possible. We thank colleagues at MRAO, and Dr Graham Woan, for useful discussions about this work, and the referee for helpful comments.

NOTE ADDED IN PROOF

An additional paper concerning the X-ray expansion of Cas A by Kovalesky et al. (1998) has recently been published.

REFERENCES

Agüeros M. A., 1997, MPhil thesis, Cambridge Univ.
Anderson M. C., Rudnick L., 1995, ApJ, 441, 307
Ashworth W. B., 1980 J. Hist. Astron., 11, 1
Bell A. R., 1977, MNRAS, 179, 573
Fesen R. A., Becker R. H., Goodrich R. W., 1988, ApJ, 329, L89
Green D. A., 1988, in Roger R. S., Landecker T. L., eds, Supernova Remnants and the Interstellar Medium. Cambridge Univ. Press, Cambridge p. 51
Gull S. F., 1973, MNRAS, 161, 47
Gull S. F., 1975, MNRAS, 171, 263
Kamper K. W., van den Bergh S., 1976, ApJS, 32, 351
Kovalesky B., Rudnick L., Gotthelf E. V., Keohane J. W., 1998, ApJ, 505, L27
McGilchrist M. M., Baldwin J. E., Riley J. M., Titterington D. J., Waldram E. M., Warner P. J., 1990, MNRAS, 246, 110
Rees N. P., 1989, PhD thesis, Cambridge Univ.
Strom R. G., Goss W. M., Shaver P. A., 1982, MNRAS, 200, 473
Tan S. Z., Gull S. F., 1985, MNRAS, 216, 949
Tuffs R. J., 1986, MNRAS, 219, 13
van den Bergh S., Dodd W. W., 1970, ApJ, 162, 485
Vink J., Bloemen H., Kaastra J. S., Bleeker J. A. M., 1998, A&A, 339, 201
Woltjer L., 1970, in Habing H. J., ed., Interstellar Gas Dynamics. Reidel, Dordrecht p. 229

This paper has been typeset from a TEX/LATEX file prepared by the author.